IV International Conference on Computational Methods for Coupled Problems in Science and Engineering
COUPLED PROBLEMS 2011
M. Papadrakakis, E. Oñate and B. Schrefler (Eds)

HIGHER ORDER TIME INTEGRATION SCHEMES FOR THERMAL COUPLING OF FLOWS AND STRUCTURES

V. Kazemi-Kamyab * †, A.H. van Zuijlen† AND H. Bijl†

†Aerodynamics Section
Faculty of Aerospace Engineering
Delft University of Technology
P.O. Box 5058, 2600 GB Delft, The Netherlands
* Email: v.kazemikamyab@tudelft.nl

Key words: Higher Order Implicit Time Integration, IMEX, Partitioned Method, Conjugate Heat Transfer

Abstract. The application of higher order implicit time integration schemes to conjugate heat transfer problems is analyzed with Dirichlet-Neumann as the decomposition method. In the literature, only up to second order implicit time integration schemes have been reported while there is a potential for gaining computational efficiency using higher orders. For loose coupling of the domains, the IMEX scheme consisting of the ESDIRK scheme for integrating the governing equations within the subdomains and an ERK scheme for explicit integration of the explicit coupling terms is utilized. The IMEX scheme is analyzed for two cases. In one, the material properties of the coupled domains are the same and in the other they are different. While for both cases, the IMEX scheme preserves the design order of the time integration scheme, different stability and accuracy properties are observed for the two. Finally, the computational efficiency of the higher order IMEX schemes relative to the second order θ scheme is demonstrated using a test case in 2-D involving coupled conduction problem of three domains.

1 INTRODUCTION

Thermal interaction of flows and structures, also known as conjugate heat transfer, arises in many engineering disciplines such as aerospace (turbine blades in jet engines), manufacturing (continuous casting), and MEMS (cooling of electronic chips). In order to obtain a better understanding of the physics of the coupled problem and hence to increase the efficiency and/or safety of the designs, numerical simulation servers as a viable tool. However, accurate numerical solution of transient conjugate heat transfer problems (CHT) can be time consuming and thus methods to achieve the desired accuracy with less computational work is of great importance.

To improve computational efficiency, higher order implicit time integration schemes as opposed to the traditionally used 1^{st} and 2^{nd} order implicit schemes are investigated. For this purpose, a family of multi-stage implicit Runge-Kutta schemes (IRK) is analyzed which can be made of arbitrary higher order while retaining robustness (stability) and efficiency. For partitioned solve of the domains, the Dirichlet-Neumann decomposition is used to tackle the spatial coupling of the domains and for time integration a higher order mixed implicit-explicit (IMEX) scheme similar to one in [1] (used for partitioned solve of the mechanical coupling of flows and structures) is considered. In the application of the higher order IMEX schemes to the loose partitioned solve of the CHT problem, the time integration's design order preservation, their efficiency relative to lower order schemes, and their stability are investigated. In particular, their behavior (stability and accuracy) is analyzed for two cases. In one, the material properties of the coupled domains are the same and in the other they are different.

2 MODEL PROBLEM

In order to investigate the properties of the numerical algorithm for thermal coupling of the domains, a model problem consisting of the one dimensional transient heat conduction in two sub-domains $\Omega_1 = [-1, 0]$ and $\Omega_2 = [0, 1]$ which are separated by the common interface Γ at $x = 0$ is considered. The two subdomains can have the same or different material properties. For simplicity, it is assumed that the material properties of each sub-domain (k thermal conductivity, c_p heat capacity, and ρ density) are constant. The governing equation within each subdomain is given by:

$$(\rho c_p)_1 \frac{\partial T_1}{\partial t} = -\frac{\partial}{\partial x}(-k_1 \frac{\partial T_1}{\partial x}) \qquad -1 \leq x \leq 0, \tag{1}$$

$$(\rho c_p)_2 \frac{\partial T_2}{\partial t} = -\frac{\partial}{\partial x}(-k_2 \frac{\partial T_2}{\partial x}) \qquad 0 \leq x \leq 1. \tag{2}$$

The non-interface boundaries at $x = \pm 1$ are insulated. For a well-posed problem, the continuity of the temperature and heat flux is imposed at the common interface of the domains, $x = 0$.

$$T_1(\Gamma) = T_2(\Gamma), \tag{3}$$

$$-k_1 \frac{\partial T_1}{\partial x}|_\Gamma = -k_2 \frac{\partial T_2}{\partial x}|_\Gamma. \tag{4}$$

3 IMPOSING INTERFACE BOUNDARY CONDITIONS

To solve the coupled problem, domain decomposition method, in particular the Dirichlet-Neumann (D-N), is used where the global domain $\Omega = [-1, 1]$ is split into Ω_1 and Ω_2. The Dirichlet (temperature) condition is assigned to Ω_2 with the interface temperature

of Ω_1 being prescribed as its value and the Neumann (the flux) condition to Ω_1 with the interface heat flux of Ω_2 being prescribed as its value thus satisfying the two interface conditions in Eqn.(3) and Eqn.(4).

In the partitioned approach, the stability of the coupling algorithm depends on the correct assignment of the interface conditions to the subdomains. Henshaw [2] analyzed the stability and rate of convergence of the interface iterations with the space kept continuous, and with the θ scheme for time integration and arrived at a criteria for imposing the interface conditions. With reference to the assigned interface boundary conditions in the model problem considered here, the criteria is:

$$|R| \approx \frac{k_2}{k_1}\sqrt{\frac{\alpha_1}{\alpha_2}} \tag{5}$$

The assigned interface boundary conditions are stable if $R \leq 1$, otherwise the two conditions must be interchanged. Here, it is assumed that, based on the material properties of the two subdomains, the imposed interface boundary conditions (Dirichlet condition imposed on Ω_2 and Neumann condition on Ω_1) satisfy the criteria. Based on Eqn.(5), when the sub-domains have similar material properties $R \approx 1$, the Dirichlet-Neumann formulation will encounter difficulties and convergence rate of the interface iterations is slow. However, when the material properties of the two subdomains are far apart, $R << 1$, the interface iterations converge rapidly.

4 SEMI-DISCRETE FORM

To solve the coupled PDE, space and time are discretized separately, with the space being discretized first in order to arrive at the semi-discrete form of the coupled problem. With reference to the imposed interface boundary conditions, in the case of coupling a fluid and a solid, typically $\Omega_s = \Omega_1$ and $\Omega_f = \Omega_2$. Therefore, following a common practice, Ω_1 is discretized using linear-basis finite elements (FEM) and Ω_2 using cell centered finite volumes (CFV) (see Fig.(1)). This combination of space discretizations for thermal coupling of the domains has been in used in the literature (for example see [3]). With the space discretized, the interface boundary conditions for the subdomains are evaluated, Eqn.(6) and Eqn.(7).

$$T_{2,1/2} = T_{1,0}, \tag{6}$$

$$q_{1,0} = -\frac{k_{2,1}}{\frac{\Delta x_{2,1}}{2}}(T_{2,1} - T_{2,1/2}). \tag{7}$$

The two equations are essentially the discrete form of the interface conditions Eqn.(3) and Eqn.(4). In order to present the model problem in matrix form, for simplicity, the

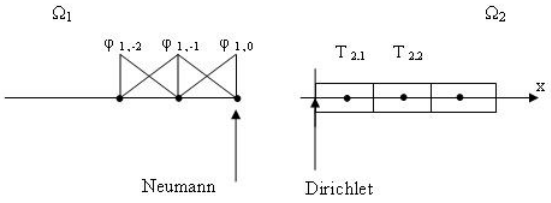

Figure 1: Discretization of the computational domain using FEM-FVM

interface temperature of Ω_2 is directly expressed by the interface node of Ω_1. Therefore, using Eqn.(6), Eqn.(7) can be expressed by:

$$q_{1,0} = -\frac{k_{2,1}}{\frac{\Delta x_{2,1}}{2}}(T_{2,1} - T_{1,0}) = S_1' T_1 + S_{12} T_2. \tag{8}$$

The expression on RHS of Eqn.(8) is the matrix representation of $q_{1,0}$ based on the nodal temperatures of the two domains. Since $q_{1,0}$ is defined at the interface, the matrices S_1' and S_{12} contain mainly zero entries (for this 1-D problem, each has only one non-zero entry). For the two sub-domains after discretization in space, the following two coupled semi-discrete forms are obtained:

$$\frac{d}{dt}(M_1 T_1) = S_1 T_1 + S_1' T_1 + S_{12} T_2 + b_1 \qquad , \tag{9}$$

$$\frac{d}{dt}(M_2 T_2) = S_2 T_2 + S_{21} T_1 + b_2 \qquad . \tag{10}$$

T_1 and T_2 are vectors containing the unknown temperature nodes, M_1 and M_2 diagonal matrices (mass-matrix), S_1 and S_2 are sparse tridiagonal matrices (stiffness matrix) and b_1 are b_2 are vectors containing the non-interface boundary terms. $S_{21}T_1$ represents the interface temperature assigned to Ω_2. Similar to S_1' and S_{12}, S_{21} contains only one non-zero entry for this 1-D test case.

5 TIME INTEGRATION

By applying a time integration scheme to the semi-discrete systems Eqn.(9) and Eqn.(10), a fully discrete system of the coupled problem can be obtained. Here, the higher order implicit ESDIRK schemes which are L-stable are considered. The L-stability property is desired since it allows for robust and stable treatment of stiffness within the system and thus the time step is restricted by accuracy rather than stability. For an ODE system of the form $\frac{dT}{dt} = \mathcal{F}(T, t)$, the solution at each stage of the ESDIRK scheme is evaluated by:

$$T^{(k)} = T^n + \Delta t \sum_{i=1}^{k} a_{ki} \mathcal{F}^{(i)} \qquad , \tag{11}$$

with a_{ki} the coefficients of the corresponding stage. High order solution at the next time level can be achieved by the weighted sum of the residual functions such that the lower order errors cancel out:

$$T^{n+1} = T^n + \Delta t \sum_{i=1}^{s} b_i \mathcal{F}^{(i)} \quad , \tag{12}$$

where b_i are the weight factor with $\sum_i b_i = 1$.

5.1 Partitioning

In the monolithic approach all the interface terms are evaluated implicitly, however, in the partitioned method some or all of the interface terms are treated explicitly, depending on the arrangement with which the two solvers are solved. Following [1], an Additive Runge-Kutta scheme is used which consists of an Explicit first stage, Singly Diagonally Implicit Runge-Kutta (ESDIRK) scheme for integrating the governing equations within the subdomains and an ERK scheme for explicit integration of explicit coupling terms and hence referred to as an IMEX scheme. For the IMEX scheme considered here, the stage coefficients given in [4] are used. The coefficients of the implicit ESDIRK scheme are denoted by a^I_{ki} and that of the ERK scheme by a^E_{ki} and both the schemes have the same weight factors b_i. Here, the coupled system is solved using the block Gauss-Seidel with integrating first Ω_2 (GS-21). The solution to the temperature field in Ω_2 at stage k, $T_2^{(k)}$, using the IMEX scheme is given by:

$$\left(M_2 - \Delta t a^I_{kk} S_2\right) T_2^{(k)} = E_2^{(k)} + \Delta t a^I_{kk} (S_{21} T_1)^* + \Delta t a^I_{kk} f_2^{(k)} \quad , \tag{13}$$

with

$$E_2^{(k)} = M_2 T_2^n + \Delta t \sum_{i=1}^{k-1} a^I_{ki} (S_2 T_2 + S_{21} T_1 + f_2)^{(i)} \quad . \tag{14}$$

Now using the updated solution field in Ω_2, $T_1^{(k)}$ is computed:

$$\left(M_1 - \Delta t a^I_{kk} S_1\right) T_1^{(k)} = E_1^k + \Delta t a^I_{kk} (S_{12} T_2)^{(k)} + \Delta t a^I_{kk} (S_1' T_1)^* + \Delta t a^I_{kk} f_1^{(k)} \quad , \tag{15}$$

with

$$E_1^{(k)} = M_1 T_1^n + \Delta t \sum_{i=1}^{k-1} a^I_{ki} (S_{12} T_2 + S_1' T_1 + S_1 T_1 + f_1)^{(i)} \quad . \tag{16}$$

E_1 and E_2 represent the known contributions from the previous stages and/or step and $(S_{21}T_1)^*$ and $(S_1'T_1)^*$ are the coupling terms that need to be predicted. The choice of the predictor must be such that the design order of the time integration scheme is preserved -without the use of sub-iterations. Since the coupled problem is linear, only T_1^* needs to be predicted which following [1] is given by:

$$T_1^* = \sum_{i=1}^{k-1} \frac{a_{ki}^E - a_{ki}^I}{a_{kk}^I} T_1^{(i)} \quad , \tag{17}$$

The solution at the next time step is obtained by applying Eqn.(12) to each subdomain (noting that for this 1-D test case, M_1 and M_2 are constant):

$$T_1^{n+1} = T_1^n + \Delta t \sum_{i=1}^{s} b_i M_1^{-1} (S_{12} T_2 + S_1' T_1 + S_1 T_1 + f_1)^{(i)} \tag{18}$$

$$T_2^{n+1} = T_2^n + \Delta t \sum_{i=1}^{s} b_i M_2^{-1} (S_{21} T_1 + S_2 T_2 + f_2)^{(i)}. \tag{19}$$

In practice where two separate solvers are used, in Eqn.(17), T_1 is replaced with the interface nodes (for the 1-D problem considered here with $T_{1,0}$). In addition, to use the IMEX scheme, the solution field of the computed stage must be stored for evaluating the later stages and the solution to the time step.

The IMEX scheme introduced will be applied to two cases of $R << 1$ and $R = 1$.

6 RESULTS

The model problem described is used to assess the the accuracy and stability of the higher order IMEX scheme. The length of each subdomain is unit meter. Ω_1 is discretized using 256 elements, and Ω_2 with 256 cells. A step initial condition is imposed on the global domain: $T_i \in \Omega_1 = -1$ and $T_i \in \Omega_2 = 1$. Block Gauss-Seidel integrating Ω_2 first, GS-21, is used to solve the coupled system. As Table.(1) shows two sets of material properties are used. Even though Eqn.(5) is used to approximate the rate of convergence of the interface iterations for the θ scheme, as it will be demonstrated, it can also be used as means to estimate whether loose coupling of the domains using IMEX will encounter any difficulties.

Table 1: Model problem material properties

Set	Subdomain	$k(W/mK)$	$\rho c_p(J/m^3K)$	R
1	1	25	5000*500	.05
	2	0.025	1000*1	
2	1	25	5000*500	1
	2	25	5000*500	

To evaluate the differences between the two cases, the partitioning error is investigated. In this model problem, the two sources of error in the partitioned solution are the

partitioning and time integration errors. The partitioning error is defined as the difference between the partitioned and monolithic solutions both computed with the same time step. The time integration error is evaluated by computing the difference between the monolithic solution obtained using a certain time step and the temporally exact solution. The temporally exact solution was acquired by solving the coupled problem monolithically using a fine time step, here $\Delta t = 0.01$ sec. When the partitioned error is below the time integration error, the dominant source of error in the partitioned solution is the time integration error.

6.1 Case of $R << 1$

Fig.(2(a)) shows the convergence plot of the partitioning error of the third and fourth order IMEX schemes (denoted by IMEX3 and IMEX4). In addition, the convergence plot of time integration errors are shown. The partitioning error of the IMEX schemes, in the asymptotic range, have the same order as their corresponding time integration errors, thus allowing the partitioning solution to have the design order of the time integration scheme. For IMEX3, the 3^{rd} order slope is observed more clearly if smaller time steps are considered. The figure also shows that when previous stage solution is used as predictor for the explicit coupling terms, reduction to second order (the stage order) is observed.

For IMEX3, the partitioning error is below the time integration error for all the time steps considered here. For IMEX4 it is above the time integration error in the asymptotic range. It should be noted that for both schemes, as the gird is further refined the partitioning error increases and for IMEX3 eventually moves above the time integration error. As it will shown later, for a 2-D test case the partitioning errors for both schemes are above the time integration error at rather coarse grids. In such cases, subiterations (or interface iterations) might need to be performed in order to increase the accuracy of the partitioned solution. A question that arises is whether gain in computational efficiency relative to second order time integration schemes is observed when the higher order ESDIRK schemes with subiterations are used for the partitioned solve of the domains.

An important behavior of the higher order IMEX schemes that is observed in their application to cases where $R << 1$ is that the solution remains stable even for time steps on the order of the time scale of diffusion within the problem (for this test case, estimated by $t_d \propto \frac{L_1^2}{\frac{k_1}{\rho_1 c_{p,1}}} = 10^5$), even though they are partly explicit.

6.2 Case of $R = 1$

Fig.(2(b)) shows the convergence plot of the partitioning error for the third and fourth order IMEX schemes for $R = 1$. In addition, the time integration errors of the third and fourth order ESDIRK schemes are also plotted. Just as in the case of $R << 1$, the IMEX schemes preserve the design order of the time integration for $R = 1$ in the asymptotic range. For both the IMEX schemes, the partitioning errors are above their respective time integration errors and in comparison to their counterparts in the $R << 1$, they

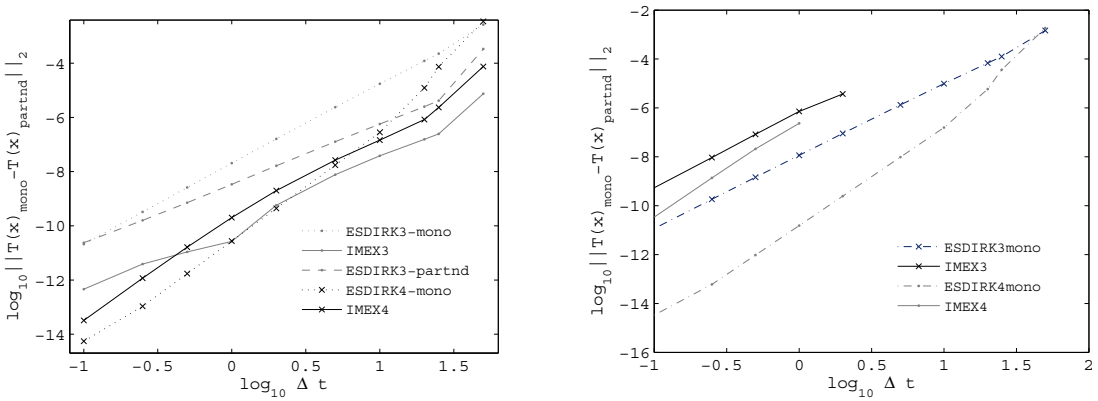

(a) (b)

Figure 2: Convergence plot of the partitioning and time integration errors for 3rd and 4th order schemes for case of (a) $R << 1$ and (b) $R = 1$.

are larger. Thus, by comparing the behavior of the schemes in the asymptotic range, one can conclude that as R approaches unity, the influence of the partitioning error on the partitioned solution becomes more noticeable, causing the larger deviation of the partitioned solution from the monolithic one.

Referring to Fig.(2(b)), it is noted that the partitioning errors of the IMEX schemes are shown only up to a maximum time step of $\Delta t = 2$, since above it the partitioned schemes are unstable. This is another important difference in the application of the IMEX schemes to the two cases. Such instabilities are not present in the monolithic solution- by observing the time integration error, and their appearance in the IMEX schemes are due to IMEX schemes' partly explicit nature. For this test case, where the material properties and the mesh spacing of the two domains are the same, instability occurs when the Fourier number of the domains exceeds $Fo = Fo_1 = Fo_2 = 1$. Thus, when the loosely coupled higher order IMEX schemes are used for time integration of cases where $R \approx 1$, the time step size choice is severely reduced, compared to the time step that can be selected independently for each domain, due to stability reasons. In order to stabilize the algorithm, subiterations must be performed.

6.3 Efficiency of the higher order IMEX scheme

When analyzing the thermal coupling of typical fluids and solids, it is observed that $R << 1$. For example for steel-air $R \approx 0.07$, and for water-copper $R \approx .0013$. Thus, the loosely-coupled IMEX scheme can be used for time-stepping the coupled problem without encountering any stability issues. However, in comparison to first order BDF1 and second order time integration schemes such as the θ scheme or BDF2 where only one implicit solve at each time step is performed, the higher order IMEX schemes, with s number of stages, computes $s - 1$ implicit solves at each time step. Therefore, the issue that

Table 2: Set of parameters used in analyzing the model problem, N : number of cells

Subdomain	L_x	L_y	N_x	N_y	k	ρc_p
Ω_1	.5	.5	20	10	54	7400×475
Ω_2	.5	.5	20	20	.06	1000×1
Ω_3	.5	.5	20	10	54	7400×475

needs to be considered is whether the higher order IMEX schemes are computationally more efficient than the lower order schemes in acquiring a certain accuracy. In that respect, the computational work of third and fourth order IMEX schemes are compared to that of the θ scheme using the model problem depicted in Fig.(3(a)) where thermal coupling of 3 domains in 2-D is considered. The governing equation within each domain is transient conduction. The outer boundaries are insulated. In the previous sections, the application of the IMEX schemes to the combination of FEM-CFV grids was shown. In this section, the IMEX schemes is used for time-stepping the coupled subdomains where all the subdomains are discretized using cell-centered finite volumes. In order to use the D-N formulation, an approximation to the interface temperature is then required. Here, this is obtained based on equating one-sided differences to compute the interface heat flux (see [5] for derivation). The material properties, the size of each domain, and the number of cells used to discretize each domain, are shown in Table.(2). With reference to the material properties shown in Table.(2), for a stable time-stepping of the coupled problem, Ω_2 takes the Dirichlet condition at the two interfaces, while the other two subdomains take the flux condition. The following initial condition was imposed on the global domain: $T_i(\mathbf{x}) = 0$ for $(\mathbf{x}) \in \Omega_i$ with $i = 1, 3$ and $T_2(\mathbf{x}) = \begin{cases} 1 & \text{if } x \leq 0.25 \\ 0 & \text{if } x > 0 \end{cases}$. The simulation were carried out to $t_{final} = 1000$ sec.

Figure 3(b) shows the total error of the partitioned solution using the IMEX scheme against the work, where work is defined as the total number of implicit stage calculations during the simulation ($W = (s-1) * \frac{t_{final}}{\Delta t}$). The total error of the partitioned scheme is obtained by comparing the partitioned solution field to its corresponding temporally exact solution field and taking the L_2 norm of the difference. The temporally exact solution was obtained using the fourth order ESDIRK and $\Delta t = 0.01$ sec. Furthermore, the results are depicted for two possible sequences with which coupled problem can be solved. The work of the second order θ scheme is also plotted as reference.

As Fig.(3(b)) shows, even in the case where an approximation to the interface equation has to be introduced to solve the coupled problem, the IMEX schemes preserve their respective design order in the asymptotic range. This result is irrespective of the sequence with which the subdomains are integrated. However, comparing the total error convergence curves for the two different integration sequences it is noted that the inte-

gration sequence does influence the magnitude of the partition error and hence the total error. After performing some numerical tests, it was observed that the magnitude of the difference depends on parameters such as the initial condition and the outer boundaries imposed on the global domain, the mesh ratio of the coupled domains, and the duration of the computations, t_{final}, and therefore a general conclusion in selecting the sequence which will always give the lowest partition error cannot be made.

For this test case, since the results, for both the θ and IMEX schemes, are not influenced noticeably by the order with which the domains are integrated, the following is true for both the integration sequences considered here. Since the governing equation within all the subdomains is transient conduction, a rough estimate of the time step to accurately capture the transients based on a Fourier number of unity is $\Delta t \approx \frac{\Delta x^2}{\alpha} = \frac{(0.5/20)^2}{.06/(1000)} \approx 10sec$. For the θ scheme with $\Delta t = 10$, the computational work performed to arrive at $t_{final} = 1000sec$ is approximately 100 and the accuracy of the solution is $\approx 10^{-5.5}$. Even though the 3^{rd} and 4^{th} order IMEX schemes require respectively 3 and 5 implicit solves per time step compared to the partitioned θ scheme, to arrive at the same accuracy the amount of work required by them are roughly 1.6 and 2.5 times less than θ scheme (for this particular test case).

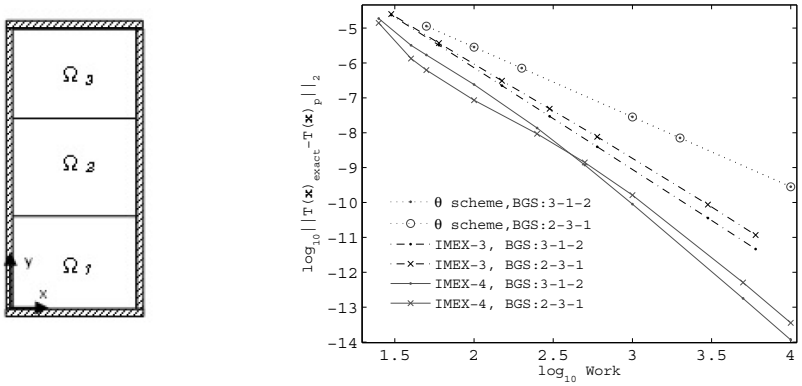

(a) (b)

Figure 3: (a) Three domains thermally coupled, (b) Comparison of the computational work of the higher order IMEX and the 2^{nd} order θ scheme.

7 CONCLUSIONS

- The higher order implicit ESDIRK schemes were used to solve thermally coupled domains with Dirichlet-Neumann as the decomposition method. For loose coupling of the domains, the IMEX scheme consisting of the ESDIRK scheme for integrating the governing equations within the subdomains and an ERK scheme for explicit integration of the explicit coupling terms was utilized. The stability and accuracy

of the IMEX scheme was evaluated for two cases: In one, the material properties of the coupled domains are quite different ($R << 1$) and in the other they are the same ($R = 1$). For both cases, in the asymptotic range, the IMEX schemes preserved the design order of the time integration scheme. However, it was observed that in comparison to $R << 1$, for $R = 1$ the influence of the partitioning error on the partitioned solution becomes more noticeable, causing the larger deviation of partition solution from the monolithic one. Furthermore, while for $R << 1$, the IMEX schemes did not encounter any stability issues for relatively small time steps (compared to the time scale of diffusion in the problem), for $R = 1$ instabilities do appear at such time steps. For the considered test case, instability occurred when the Fourier number of the domains exceeded unity, $Fo = Fo_1 = Fo_2 > 1$. To stabilize the algorithm, subiterations must be performed.

- The computational efficiency of the higher order IMEX schemes relative to the partitioned second order θ scheme was considered using a test case in 2-D involving coupled conduction problem of three domains. Even though greater number of implicit solved per time step is required for the IMEX schemes compared to the θ scheme, it was demonstrated that to arrive at the same accuracy, the IMEX schemes required less computational effort.

REFERENCES

[1] van Zuijlen, A.H. and Bijl, H. Implicit and explicit higher order time integration schemes for structural dynamics and fluid-structure interaction computations. *Computers and Structures.* (2005) **83**:93-105.

[2] Henshaw, W.D. and Chand, K.K. A composite grid solver for conjugate heat transfer in fluid-structure systems. *Journal of Computational Physics.* (2009) **228**:3708-3741.

[3] Roe, B. Haselbacher, A. and Geubelle, P.H. Stability of fluid-structure thermal simulations on moving grids. *International Journal for Numerical Methods in Fluids.* (2007) **54**:1097-1117.

[4] Kennedy, C.A. and Carpenter, M.H. Additive Runge-Kutta schemes for convection-diffusion-reaction equations. *Applied Numerical Mathematics.* (2003) **44**:139-181.

[5] Carlson, K.D. Lin, W.L. and Chen, C.J. Pressure Boundary Conditions of Incompressible Flows with Conjugate Heat Transfer on Nonstaggered Grids Part II: Applications. *Numerical Heat Transfer, Part A.* (1997) **32**:481-501.